SLD Optical Sensing Applications

Takashi Nakayama

[Summary] Use of optical sensing technology is spreading rapidly in medical, industrial, and process measurement fields. The super luminescent diode (SLD) is used by these systems for products in a wide price range. Anritsu's SLD modules featuring wide bandwidth, low coherence, and high output power are ideal for use as optical-sensing light sources. This article explains the principles of the SLD as well as the features of each wavelength and presents some interference measurement results. It also introduces application examples of optical coherent tomography (OCT) in the medical field, atomic force microscopy in the industrial field, and sensing using a Fiber Bragg Grating (FBG).

1 Introduction

Optical sensing is technology for quantitatively measuring remote targets using light. The wavelengths and time difference of returning light reflected by and scattered from the illuminated target are measured to estimate the distance to the target as well as the thickness, surface roughness, cross-section, etc. As societies become increasingly aged, optical sensing is expected to find widespread applications in medical fields as well as in the rapid digital transformation (DX) of industry.

The Super Luminescent Diode (SLD) for optical sensing is similar to the Laser Diode (LD) but has low coherence and a wideband optical spectrum, and can be coupled with high efficiency to optical fiber.

2 SLD Basics

2.1 Comparison of Semiconductor Light Emitting Devices

Table 1 lists the features of LD, SLD, and Light Emitting Diode (LED) semiconductors emitting light from an end facet. The cross-section of each type is shown but all types have an active layer that generates light when current is injected. The LD has a reflection coating on both facets which serve as mirrors to amplify internally reflected light and the LD oscillates as a laser when the active-layer resonance gain matches the mirror loss. The spectrum half-width is narrow at less than a few nm. As described later, the coherence length ranges from several tens of centimeters to several

Table 1 Features of Each Semiconductor Light-Emitting Devices

Item	LD	SLD	LED
Light Generation	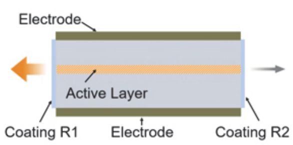 Coating Reflectivity R1 < R2	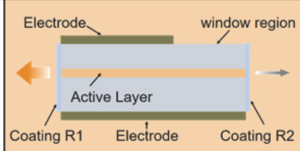 Coating Reflectivity R1=R2≒0	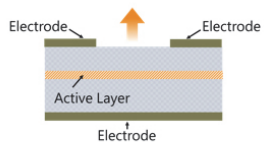
Emitted Light	Stimulated Emission	Amplified SE	Spontaneous Emission (SE)
Spectrum Half-Width	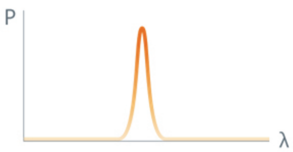 Several nm max	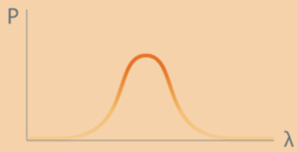 10 to 50 nm	 to 100 nm
Coherence Length	20/30 cm to several meters	10 to 80 μm	Several μm
Output Power	Several 100 mW	10 to 20/30 mW	Several mW
Fiber Coupling	○	○	×

meters and the emitted light is easily impacted by interference. A high optical output of 100 mW or more can be obtained. The internal optical waveguide carries light to the end facet from where it is emitted and can be coupled using a lens to a single mode fiber.

In comparison, the LED emits light from the surface. This spontaneous light emission has a spectrum half-width of 100 nm or more as well as a coherence length of several nm and is not easily impacted by interference. The optical output power is very low at less than a few mW and since there is no waveguide carrying the internal light, it is very difficult to couple an LED to fiber.

Although the SLD has a similar structure to the LD, the emitted internal light does not resonate because of AR coating on both facets. However, emitted light in the waveguide is amplified by amplified spontaneous emission (ASE). Although it depends on the active layer structure and chip length, the spectrum half-width is almost 10 to 50 nm and the respective coherence length is 10 to 80 µm, while the optical output is 10 to several tens of mW. In other words, the SLD optical output and spectrum half-width are positioned between the LD and LED but the SLD ease of fiber coupling is on par with the LD.

2.2 SLD Chip Structure

Figure 1 shows the structure of the Anritsu SLD chip. The crystal is grown using metalorganic vapor phase epitaxy (MOVPE) and the active layer uses a multi-quantum well (MQW) structure. The substrates are GaAs for the short-wavelength (1.1 µm max.) SLD, and InP for the long-wavelength (1.2 µm min.) SLD.

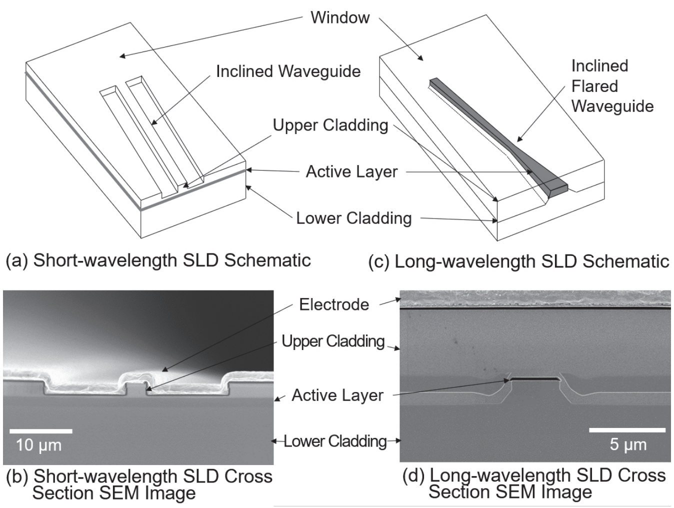

Figure 1 SLD Chip Structure

To control the SLD internal light oscillation, the reflectivity of the chip end facets must be kept as low as possible, so both are AR-coated using a dielectric film, but the reflectivity is still limited to about 0.1%. This reflectivity is the probability that light reflected by the facets is recoupled to the waveguide; to reduce reflectivity, a window region without a waveguide is fabricated near the back facet along with an inclined waveguide structure[1), 2)]. The effective facet reflectivity is held to an extremely low 0.005% by this complex design, preventing internal light oscillation.

2.3 SLD Optical Output

Figure 2 shows a schematic for the short-wavelength SLD light emission. Injecting current to the active layer causes spontaneous light emission at the active layer. This spontaneously emitted light is amplified by injecting current into the waveguide at an electrode in the waveguide, resulting in emission of ASE light from the front facet. Light passing in the waveguide towards the back facet is not amplified but is instead absorbed. As described in section 2.2, to suppress the SLD reflectivity as far as possible, the light is amplified as a traveling wave in a single pass without making an internal round trip in the SLD. As a result, the SLD optical output power is in the range of about 10 to several tens of mW. Since the light is generated by ASE, the spectrum half-width is wideband at 10 to 50 nm. Moreover, the spectrum ripple or spectrum amplitude, which is an error factor at interference measurement, is very low at just 1% due to the maximized reflectivity reduction at both end facets.

These features support the 30% to 50% efficiency when coupling Anritsu SLDs to single mode fiber (SMF).

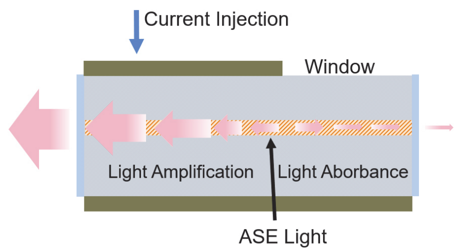

Figure 2 SLD Light Emission Schematic

2.4 Coherence

This section describes the low-coherence properties of SLDs. Figure 3 (a) shows the typical configuration of a Michelson interferometer. Light from an SLD, is split by a half-mirror into two paths. Light in the measurement path illuminates the measurement target where it is reflected back to the photodiode (PD). Light in the other reference path passes through the half-mirror to strike the reference mirror from where it is reflected back via the half-mirror to the PD. The reference mirror can be moved in the direction of the optical path to match the length of the measurement and reference path, causing interference and increasing the level. Figure 3 (b) shows this state with the x-axis representing the difference in the optical path length and the y-axis representing the coherence level. The coherence level half-width at half maximum is called the coherence length l_C and is found from Eq. (1)[3] where λc is the ASE light center wavelength, and Δλ is the spectrum half-width. As can be seen from the equation, the light becomes wideband and the coherence length becomes shorter as the spectrum half-width becomes wider, forming a low-coherence light source. Anritsu SLDs have a calculated coherence length l_C of 6 μm at λc of 840 nm and Δλ of 50 nm, indicating that there is no interference if the optical path drifts even when the SLD coherence length is extremely short.

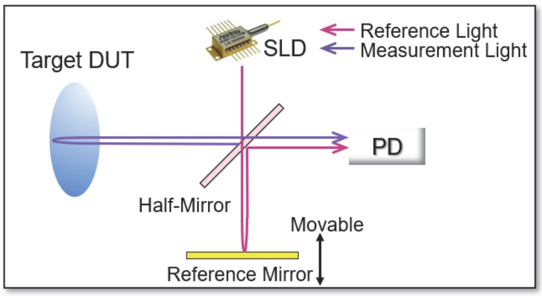

(a) Michelson Interometer

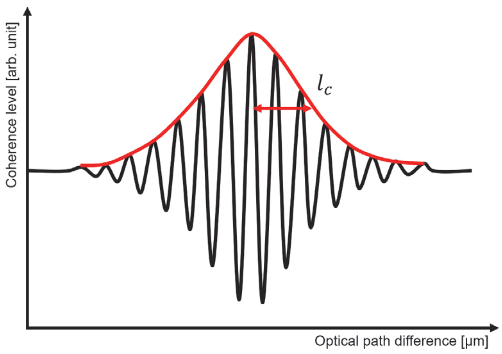

(b) Optical path Difference vs Coherence Level

Figure 3 Coherence Test

$$l_c = \frac{2ln2}{\pi}\frac{\lambda_c^2}{\Delta\lambda} \quad (1)$$

The advantage of a low-coherence SLD light source with an extremely short coherence length is that low noise interference can be measured with good resolution.

2.5 Module Structure

Anritsu manufactures three types of SLD package: butterfly module, ϕ5.6 CAN, and cylinder module. Figure 4 shows the external appearance of each type. This section describes details of the butterfly module.

(a) Butterfly Module (b) ϕ5.6 CAN (c) Cylinder Module

Figure 4 SLD Packages

Anritsu's has long experience in assembling butterfly modules for use as lasers to pump fiber amplifiers, and uses similar parts and processes to assemble SLDs. Figure 5 shows the butterfly module schematic. A chip on carrier (COC) with the SLD chip plus a PD for monitoring are soldered on a base plate along with a thermo-electronic cooler (TEC) soldered to the board back side. The lens isolator is welded to this assembly next, and then the whole is sealed under a seam-welded lid. At the last stage, the optical-fiber axis is aligned while light is being emitted from the sapphire glass window in the package edge before fixing in place. All these assembly processed are similar to those used for other optical devices and are executed on production lines using precision automatic bonding equipment.

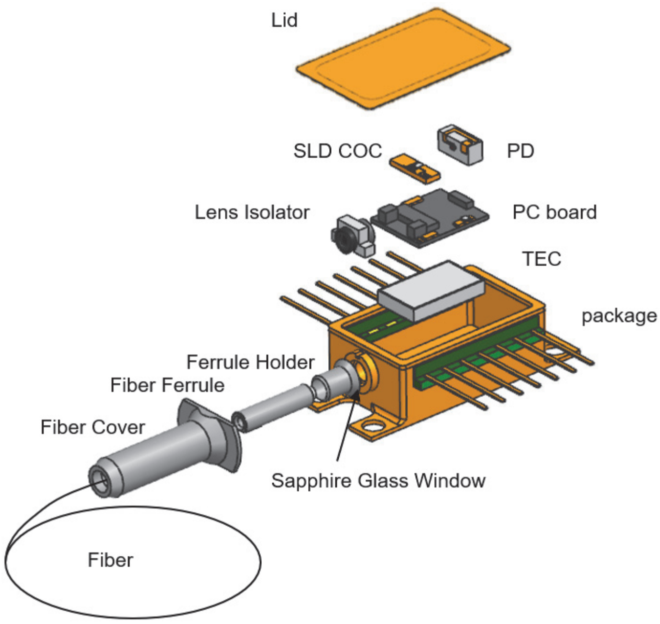

Figure 5 Butterfly Module Schematic

In addition, only long-wavelength SLD butterfly module products have the built-in isolator. Consequently, products using short-wavelength SLD and cylinder modules or the ϕ5.6 CAN require precautions about changes in characteristics caused by returning light.

3 Anritsu SLD Products

3.1 Anritsu SLD Specifications

Figure 6 shows an example of the characteristics of an Anritsu short-wavelength SLD and Figure 7 shows an example for a long-wavelength SLD; Table 2 lists the specifications of Anritsu SLD modules.

From Figure 6 (a) showing the optical output versus current characteristics, since there is no laser oscillation, there is no threshold current and the optical output is rapidly amplified. Figure 6 (b) shows the optical spectrum at 5 mW output. The spectrum waveform of a normal 0.8 µm SLD LD (AS8B115GT30M) has a single peak and the spectrum half-width defined as the width with a spectrum peak strength of 3 dB is 14 nm. On the other hand, for a wideband 0.8 µm SLD (AS8B115LT40MA) designed with an active layer to increase the gain at the short-wavelength side by increasing the current, the optical spectrum is bimodal and the spectrum half-width is wider at about 50 nm. Since coherence length gets shorter as the spectrum half-width widens, the wideband, short-wavelength SLD has excellent resolution for interference measurement.

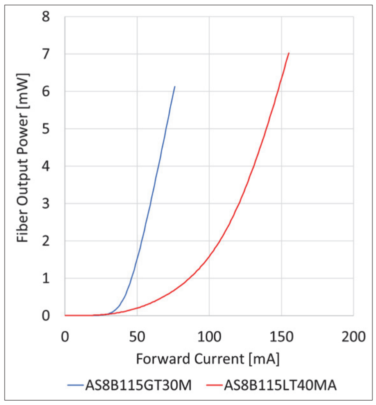

(a) Short-Wavelength SLD Optical Output vs Current Characteristics

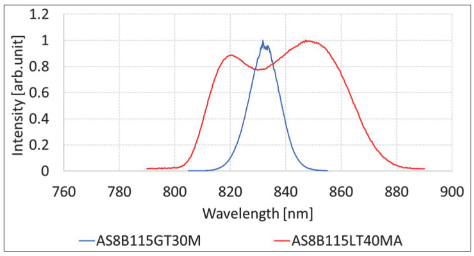

(b) Short-Wavelength SLD Optical Spectrum Characteristics

Figure 6 Short-Wavelength SLD Characteristics

Comparison of Figure 7 (a) showing the optical output vs current characteristics for a long-wavelength SLD with Figure 6 for a short-wavelength SLD indicates a high fiber optical output exceeding 10 mW at high operating currents.

As shown by the optical spectrum in Figure 7 (b), Anritsu's product line of long-wavelength SLDs cover wavelengths from 1.3 to 1.6 µm.

Our 1.55 µm SLD (AS5B310KM50M) is a lower-cost version with a lower output of 3 mW but with a similar wavelength and spectrum half-width to other products and offering about the same interference measurement resolution.

Table 2 Anritsu SLD Module Specifications

Item	Units		Short-Wavelength SLD 0.8 µm SLD		Long-Wavelength SLD 1.31 µm SLD	Long-Wavelength SLD 1.55 µm SLD		Long-Wavelength SLD 1.65 µm SLD
			AS8B115GT30M	AS8B115LT40MA	AS3B119GM10M	AS5B125EM50M	AS5B310KM50M	AS6B118GM50M
Rated Optical Output	mW	—	5	5	15	25	3 Typ	10
Forward Current	mA	Max	150	180	400	500	—	350
		Typ	—	—	—	—	200 (current rating)	—
Center Wavelength	nm	Max	810	820	1290	1530	1530	1630
		Typ	830	840	1310	1550	1550	1650
		Min	850	860	1330	1570	1570	1670
Spectrum Half-Width	nm	Typ	14	50	50	60	60	70
		Min	10	45	55	55	40	65

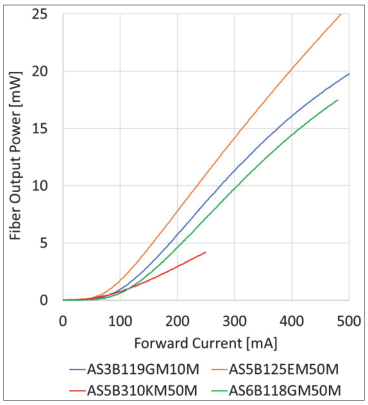

(a) Long-Wavelength SLD Optical Output vs Current Characteristics

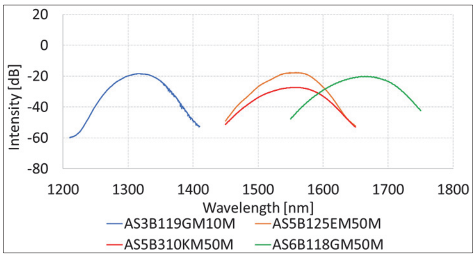

(b) Long-Wavelength SLD Optical Spectrum Characteristics

Figure 7 Long-Wavelength SLD Characteristics

The output power of SLD chips drops significantly as temperature rises, so a TEC is built into both short-wavelength and long-wavelength butterfly modules to control temperature. As a result, the SLD chip temperature remains constant whatever the external temperature to assure stable chip characteristics. The characteristics in the figures were all obtained when the chip temperature was held to 25°C.

3.2 Anritsu SLD Coherence and Reliability

Figure 8 shows the measured coherence characteristics of the AS8B115LT40MA package with optical path length difference on the x-axis and coherence level on the y-axis. The figure inset shows a magnified view of the main peak. Since Anritsu SLDs have low coherence, the coherence level falls by 3 dB with an optical path length difference of 7.7 μm, which almost matches the value found from Eq. (1) for a coherence length of 6 μm. In addition to the main peak, there are peaks that come from the reflections at the chip edges. The difference in the strengths between the main peak and next-largest peak is called the second-order coherence level. If this second-order coherence level is large, there is a lot of noise at interference measurement. When the reflection point is distance l in a medium of equivalent refractive index n_{eff}, the reflection point gap where second-order coherence occurs is found from Eq. (2)[2].

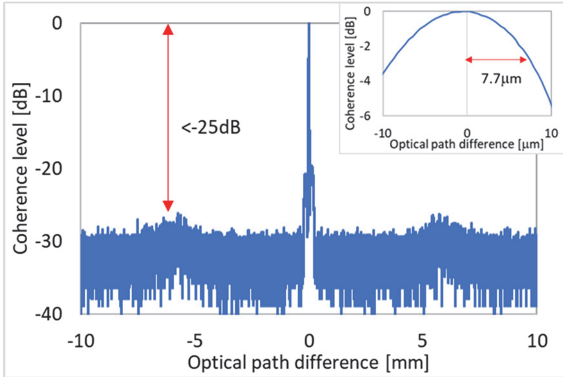

Figure 8 Coherence Measurement Results

$$L = \frac{l}{2n_{eff}} \tag{2}$$

Since the length l of the AS8B115LT40MA SLD chip is 1 mm, a second-order coherence peak is observed where L is about 7 mm, but Anritsu SLDs have measures described previously to limit end-facet reflectivity, so the second-order coherence level is very much smaller than the main peak of 25 dB max.

The next section describes reliability. Against the chip built in AS8B115LT40MA of 13 units, continuous operation test was conducted respectively for 5,000 hours at chip end facet output of 15 mW (equivalent to a fiber output of 5 mW) on constant control under ambient temperature of $T_a = 50$°C. Figure 9 shows the temperature test results with operation current I_{op} on the y-axis.

Failures occurred when the operation current was 1.2 times the initial value and the median life (ML) at $T_a = 50$°C (ML 50°C) defined as the point when cumulative failures reached 50% of the total was 30,000 hours. According to the Arrhenius relationship (Eq. 3), the chip median life at 25°C (ML 25°C) is at least 100,000 hours when the active layer is energized at 0.4 eV, which is clearly sufficient for high-reliability applications in sensing equipment.

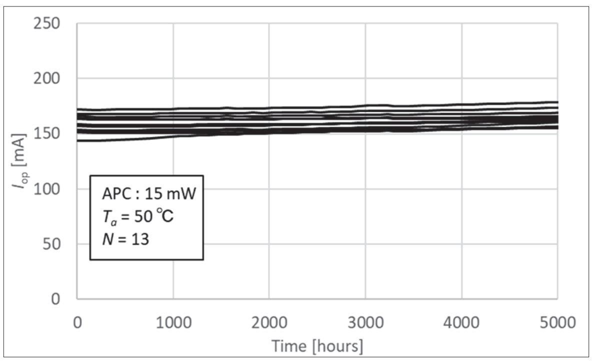

Figure 9 High-Temperature Operation Test

$$ML = A \exp\left\{-\frac{E_a}{kT}\right\} \tag{3}$$

where, k is the Boltzmann Constant and T is temperature.

Moreover, all test items in the Telcordia GR-468 CORE standard used for optical communications devices, including vibration impact, high-temperature storage, and temperature cycling, were passed without problems.

4 SLD Applications

4.1 SLD Interference Test

Interference measurement was tested using a short-wavelength SLD module. Figure 10 shows the configuration of a Michelson interferometer used for the test. It has the same optical coupler and half-mirror functions as shown in Figures 3 and 12. The light from the SLD module is divided by the optical coupler with one path illuminating the measured item (DUT) and the other passing via a polarization controller and a dispersion compensation glass plate before reflection by a mirror. Light reflected by the DUT and light reflected by the reference mirror are combined by the optical coupler and input to a spectroscope. The spectrum observed by the spectroscope when the optical path length difference is ΔL has a strong peak at λ_n satisfying Eq. (4).

$$\Delta L = n\lambda_n \qquad n = 0, 1, 2, 3 \ldots \tag{4}$$

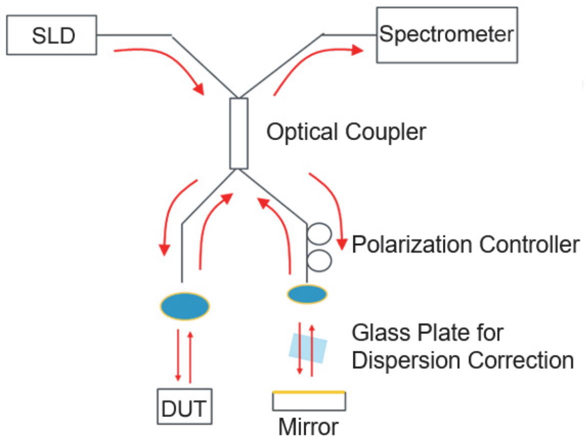

Figure 10 Interference Test Setup

Performing Fast Fourier Transformation (FFT) on this spectrum finds the distance to the DUT reflection point by calculating *ΔL*.

In addition, depth cross sections of the DUT can be obtained by scanning the lens in the DUT light path horizontally. This type of measurement is called optical coherence tomography (OCT). Figure 11 shows some actual OCT cross-section images. The image contrast indicates the reflection strength with highlights having high reflectivity. Figures 11 (a), (b), and (c) are the OCT images at the cross-section indicated by the red lines in the pictures of the leaf, onion, and feather, respectively. In (a), only the surface of the leaf has high reflectivity, while in (b) the one layer of onion has high reflectivity at the front and back faces. However, it is also possible to observer the internal layers between the faces. In (c), the shape of the feather cross-section can be seen clearly.

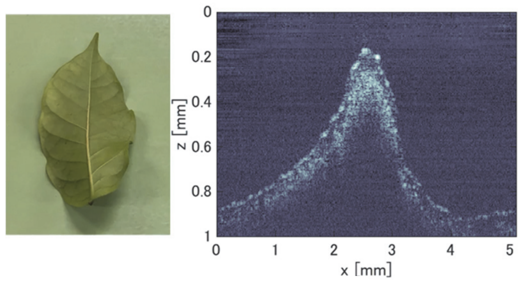

(a) Leaf Cross-Section

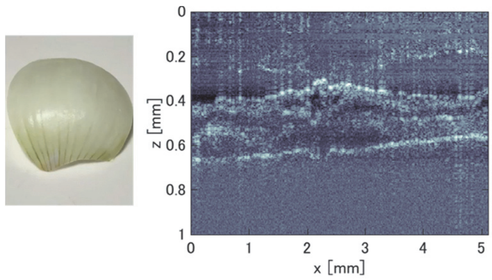

(b) Onion Cross-Section

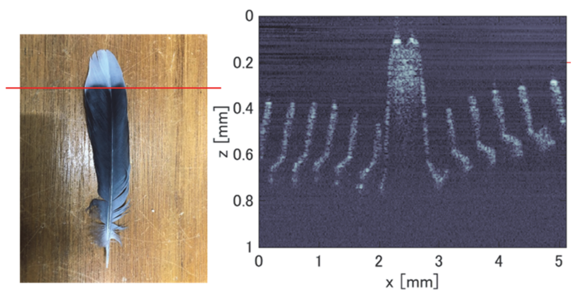

(c) Feather Cross-Section

Figure 11 Interference Test Results using SLD

4.2 SLD Medical Applications

The absorption of blood hemoglobin is larger at shorter wavelengths and smaller at wavelengths longer than 700 nm. Conversely, the absorption of water is large at wavelengths longer than 1000 nm. In this wavelength domain between 700 and 1000 nm, the absorption of both water and hemoglobin are smaller. This region is called the “optical window into the living body” and is a good wavelength domain for medical sensing applications. Consequently, ophthalmic OCT using 800-nm band SLDs is especially fruitful for observing the eye retina because its low impact on the eye is safe and precise but can detect macular degeneration and glaucoma early.

Figure 12 shows a cross-section of the retina obtained using our 0.8 µm SLD with a Spectrum Domain (SD)-OCT optical system. The light from the SLD is divided by the mirror and one light path is used to observe the eye retina while the other light path is reflected by the fixed reference mirror. The returning reflected light in both paths is combined and the interference spectrum is received at the spectrometer before signal processing as described in section 4.1 to produce a cross-section image of the retina shown in Figure 12 (b). The upper part of the cross-section image shows the vitreous humor above the neural retina over the retinal pigment epithelium, choroid membrane and retina. The light reflected by the retinal pigment epithelium is particularly strong. In addition, the eye axial length can be measured as the distance from the cornea to the fundus oculi. Conventionally, eye axial length is measured during pre-treatment testing to determine the power of the artificial lens for correcting cataracts. In addition, eye axial length is measured when testing for increasingly common myopia.

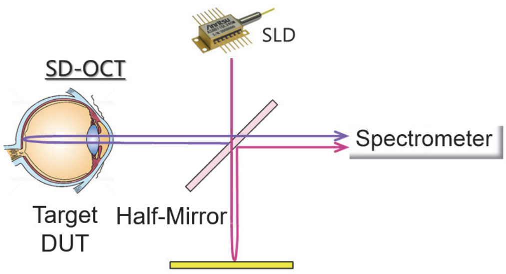

(a) SD-OCT Optical System

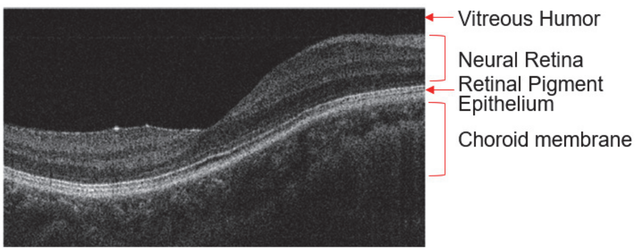

(b) OCT Cross-section of Retina

Figure 12 OCT using SLD

4.3 SLD Industrial Applications

(1) Atomic Force Microscope (AFM)

Wideband-spectrum SLDs are used to measure shapes, such as surface form and roughness. One typical application is the atomic force microscope (AFM) shown in Figure 13. The interatomic force between the probe at the tip of a cantilever and atoms at the material surface causes the cantilever to swing and this swing is measured. Illuminating the back face of the cantilever with light from an SLD detects positional displacement using light received by an optical displacement detector. The AFM can observe the surface of objects with extremely high nm-order precision.

An SLD is used as the AFM light source because it has low speckle noise, which causes optical power to oscillate due to interference between reflected light. Since high-coherence laser light is easily susceptible to interference, the light intensity fluctuates both in time and space, but low-coherence SLDs are resistant to interference and the relatively low fluctuation in light intensity permits very high-accuracy positional displacement observation.

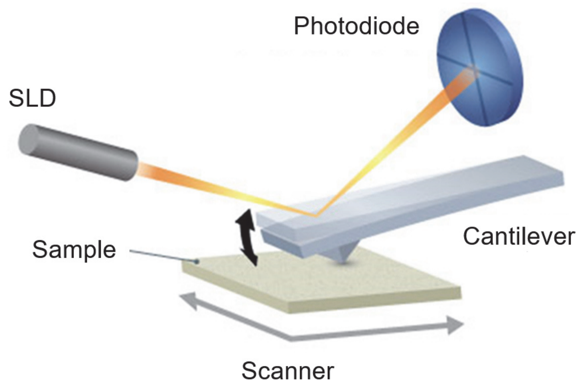

Figure 13 Atomic Force Microscope Schematic

(2) Optical Fiber Sensor

One type of optical fiber sensor called the Fiber Bragg Grating (FBG) can measure the expansion and contraction (distortion) as well as temperature of target objects using an FBG formed in a fiber. Injecting wideband light like that from an SLD into an FBG reflects and returns only light matching the grating pitch. When the refractive index of the FBG changes due to bending or temperature change, the wavelength of the reflected light also changes accordingly. Consequently, the FBG can be used to sense distortion and temperature from the wavelength of the reflected light.

An FBG sensor using an SLD was tested using the configuration shown in Figure 14 (a) by inputting light from the SLD to the FBG fiber. Reflected and returning light from the FBG passes via an optical circulator to a 64 ch arrayed waveguide grating (AWG) where it is split. This split light is received by a 64 ch PD and A/D-converted to measure the optical power of each wavelength and calculate the wavelengths of light reflected from the FBG.

The results are shown in Figure 14 (b). As shown in the inset, the FBG indicated in green is attached to the plastic plate indicated in blue. There are three gratings indicated as FBG1, FBG2, and FBG3. Any change in the distortion is measured by setting the time when a shock is added at point X to 0 s and observing changes in the light reflected from each FBG. Figure 14 (c) shows the results using a magnified time base. At the instant the shock is added, the signal at the closest FBG1 starts to change at time 0 s and then the signal at FBG2 starts changing 200 µs later followed by the signal at the most distant FBG3 400 µs later; the positional displacement of the signal permits estimation of the distance from the point X. Using this FBG sensor facilitates observation of the shock arrival time and the distortion transmission state.

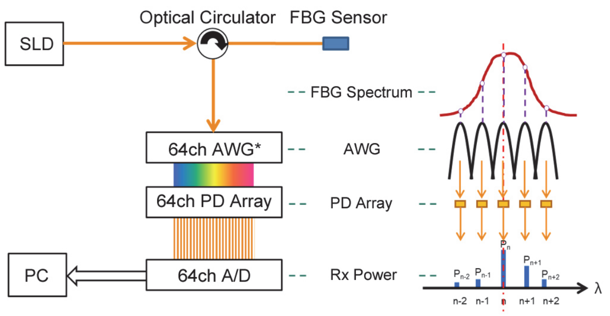

(a) Sensor Configuration

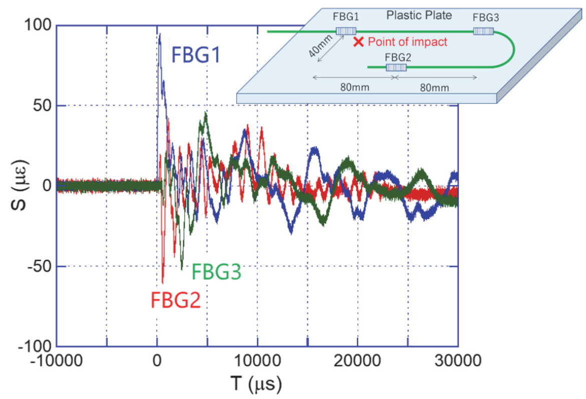

(b) FBG Sensor Measurement Results

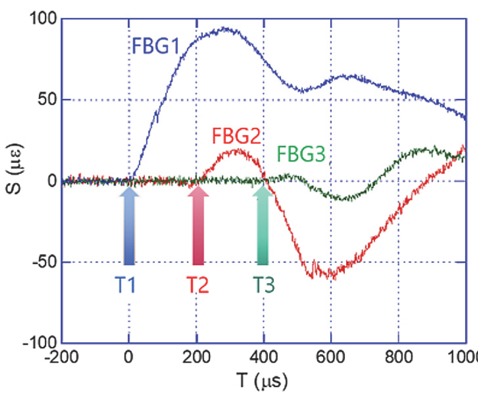

(c) Magnified FBG Sensor Measurement Results

Figure 14 FBG Sensor Test

5 Conclusions

After explaining the basic structure, principles, and some features of the SLD module, this article describes some application examples using the high output and low coherence of Anritsu's SLD product line.

Although not included here, SLDs are also used in the medical field to measure the refractive index of the eye with an autorefractometer. Other application examples in the industrial field include film thickness and displacement meters as well as optical encoders.

Supporting future market needs for high-accuracy and high-resolution sensing requires development of high-output SLD modules with a wider spectrum half-width.

References

1) H. Watanabe, H. Yoshidaya, T. Suzuki, K. Murakami, A. Yamada, K. Mise: "Development of High-power 0.8 µm SLD", Anritsu Technical Bulletin No.82 (in Japanese) (Mar. 2006), No.82, pp.59-6538777

2) A. Yamada, H. Yoshidaya, M. Fujita, S. Morimoto, T. Omatsu: "1.3 µm superluminescent diode with oblique window structure", Journal of the IEICE vol. J97-C, No. 8, pp. 308-316, 2014. (in Japanese)

3) Y. Takubo, S. Yamashita: "Research on performance improvement of dispersion-tuned fiber laser for OCT application" University of Tokyo doctoral dissertation, Dec, 2015. (in Japanese)

Authors

Takashi Nakayama
1st Development Dept.
Development Div.
Sensing & Devices Company